Correlation Structure of Ionospheric Estimation and Correction for WAAS

Andrew Hansen Eric Peterson Todd Walter Per Enge

Stanford University

ABSTRACT

The ionosphere is a distributed medium that causes dispersive delay in the propagation of transionospheric radiowaves such as GPS signals. One of the fundamental components of the Federal Aviation Administration's Wide Area Augmentation System for GPS is the estimation and correction of this geographically varying delay. Because GPS is based on satellite ranging determined by propagation time, any uncorrected advance or delay in the propagation time such as residual ionospheric delay represents an error source in the resulting differential position solution. If this residual delay exceeds the confidence bound given on the range correction the error may constitute a threat to the navigation user. Paramount in aviation applications using WAAS for navigation guidance is the protection of the position solution, whereby we mean the containment of the position error within the confidence bound in the position domain.

One approach to protecting the user from residual error in the differential navigation solution is to inflate the confidence bound on the differential range corrections which in turn inflates the confidence bound in the position domain. The penalty for taking this approach however is quite high because the system may only be used for guidance if the confidence bound on the position, which we call Horizontal and Vertical Protection Levels (HPL and VPL), are smaller than the corresponding Horizontal and Vertical Alert Limits (HAL and VAL) for any given phase of flight. In aviation applications of WAAS, the ionospheric corrections are only required for the final approach phase of flight when Instrument Precision approach with Vertical guidance (IPV) or Category I precision approach (CATI) conditions apply. These conditions have the most stringent requirements specified in the WAAS Minimum Operational Performance Standard (WAAS MOPS) and are very challenging to achieve. Thus the inflate approach is not satisfactory.

A better approach is to consider the correlation structure of the ionospheric measurements taken by the WAAS reference network and in turn the correlation structure of the residual error after the resulting ionospheric correction is applied to the user's ranging measurements. With such a characterization, the confidence bounds on the ionospheric corrections can be minimized to increase availability and yet still protect the user's navigation solution. We undertake the characterization process with real measurements from the WAAS reference station network over North America.

We have utilized both ionospheric models and real measurements to build an additive correlation model of the ionosphere which can be used in the estimation process for constructing WAAS ionospheric corrections. This correlation model is critical to the ionospheric estimator as part of the covariance propagation we use to determine the ionospheric correction confidence bounds or so-called Grid Ionospheric Vertical Error (GIVE). The paper includes a description of this model, its implementation in the correction algorithm, and an analysis of the performance achieved by the overall WAAS correction in terms of accuracy, integrity, and availability.

INTRODUCTION

Ionospheric correction in the Wide Area Differential GPS concept can be separated into three components: an estimation problem, a transmission problem, and a prediction problem [1]. The first step in the differential correction process is to construct a model of the ionosphere. Then given a set of biased and noisy measurements of ionospheric delay, the second step is to fit the model to the available measurements and generate a confidence bound on the residual error. Taken together these two steps constitute the estimation problem.

Once complete, the solution to the estimation problem at the current point in time may be encoded and sent to remote users. While not the focus of this paper, the WAAS solution to the transmission problem is both powerful and elegant. Using a state space model the WAAS separates states by their necessary update rates, the vector corrections have been condensed into a single 250bps message stream [2]. This highly efficient correction stream is suitable for transmission on practically any communication channel, most significantly geosynchronous satellite broadcast where the coverage region closely matches the service volume.

The correction information decoded from the WAAS message stream is applied by reconstructing the state estimates (ionosphere, clock, ephemeris) and projecting them onto the user's observation geometry. For the ionospheric term this is the prediction problem. In the case of the ionospheric corrections it amounts to predicting the ionospheric delay along a line-of-sight (LOS) and generating a confidence bound on the residual error between the prediction and the true delay.

It is the nature of the ionosphere that allows the differential correction concept to work. Consider the ionospheric delay along one LOS as a random process. We are only able to predict the delay on a user's observations because it is, at a minimum, correlated with the delay along other LOSs [3]. The focus of this work is to characterize the structure of that correlation. More explicitly, we seek to characterize the correlation structure of the ionosphere under the model invoked in the estimation problem.

Figure 1 depicts the typical WAAS situation where the network of GPS reference stations collects measurements (thin lines) of the ionospheric delay in order to predict the delay on the user's observations (heavy lines over the West Coast). These lines are the portion of the LOS rays from receiver to satellite that intersect the ionosphere (100-1000 km altitude). We know that a significant portion of the delay seen on the user's observations is directly correlated to the reference measurements. However, the portion which is not the same contributes directly to the residual error in the prediction. We can quantify that residual error by analyzing the correlation structure of real data through off-line processing. This information is directly applicable to the construction of the confidence bound on the residual error in the user's prediction.

There is one difficulty in identifying this correlation

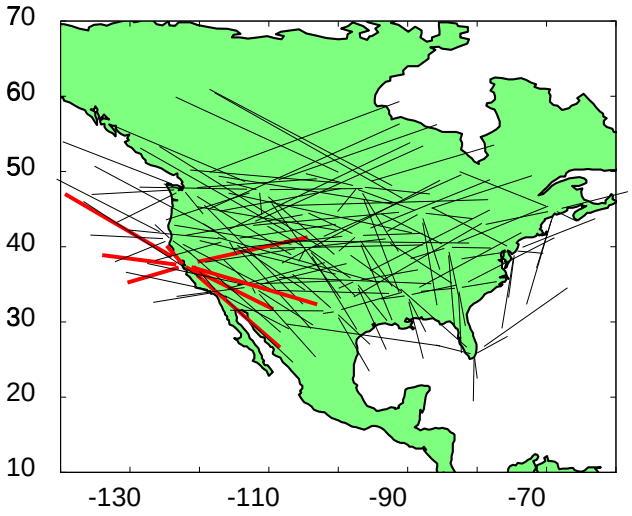

Figure 1: Reference measurements (thin lines) spatially correlated by the ionosphere are assembled into continental scale models. Correlated user observations (heavy lines over the West Coast) are corrected by projecting the model onto the local SV geometry.

structure from real data. Although many ionospheric observations are available from the GPS reference network those measurements are corrupted by noise and biases in the sensors. In our characterization we do not want to distort the ionospheric correlation by the correlation structure of these corrupting terms. By leveraging a time history of geographically redundant measurements we can average against the noise and calibrate out the biases. Once highly accurate ionospheric observations are available we can reduce the data into a correlation model.

In the remainder of this paper we will address three main topics. The first is a short description of the ionospheric model used in the estimation problem. The second is the selection and identification of a correlation model of the ionosphere using real measurements. The third is the overall performance of the differential corrections under nominal and stressful conditions that was realized by our implementation of the three (estimation, transmission, and prediction) components in the WAAS application.

IONOSPHERIC MODEL

Numerous ionospheric models have been proposed and implemented by not only the GPS community [5, 6, 7, 1] but also the atmospheric research community [8, 9] in general. They range from empirical models like IRI95 and PIM which

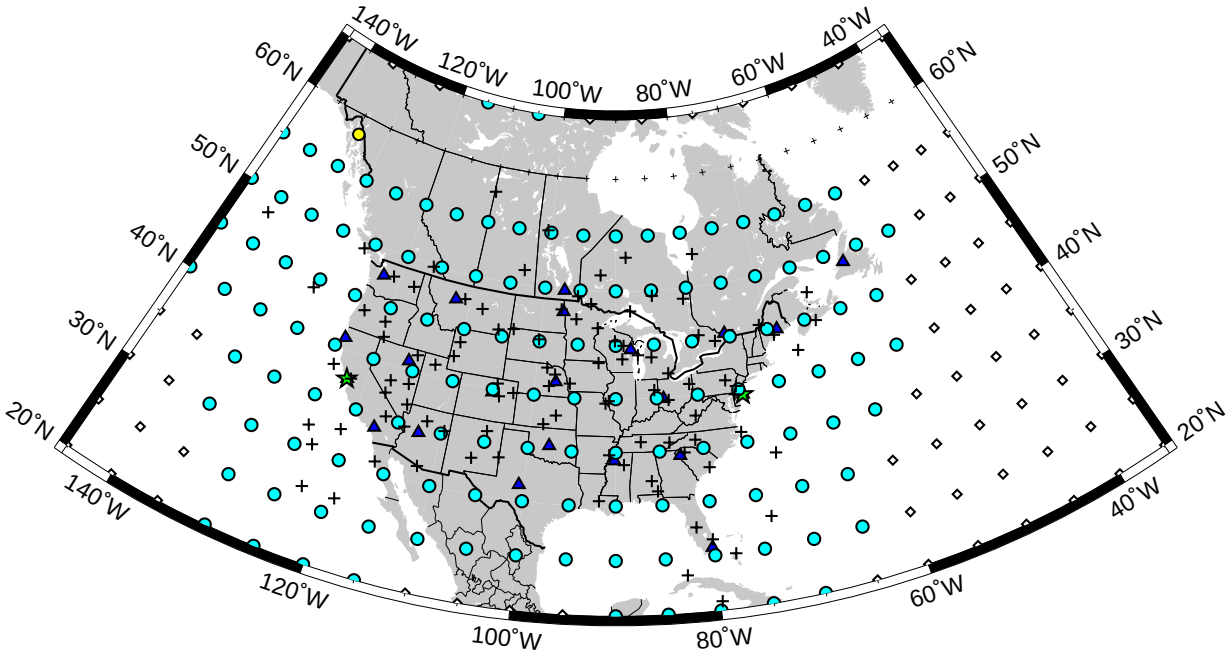

Figure 2: The ionospheric model broadcast by the WAAS consists of a thin shell at 350km altitude which is discretized into a geodetically rectangular grid. A vertical delay estimate and a confidence bound on that estimate are made at each vertex in the grid. The detailed specification of the WAAS grid can be found in the WAAS MOPS [4].

capture large scale and climatological behavior from historical data to real-time estimators that reconstruct the ionosphere from live measurements in specific locales. Likewise the collection of potential models include both two- and three-dimensional domains. As mentioned above the correlation structure we seek is effected by the model that is used to represent the ionosphere. Since we are trying to identify the correlation structure corresponding to the WAAS process we are obliged to conduct our analysis within the domain of the WAAS ionospheric model.

The basic model of the ionosphere that the WAAS has implemented is a thin-shell approximation. This collapses the variation of the ionosphere's electron density distribution into an impulse function in the radial direction. The thin-shell approximation creates a vertically equivalent ionosphere that varies only with latitude, longitude, and time. The transformation is carried out by a non-linear mapping called the obliquity factor. In its simplest form the obliquity factor is a dimensionless quantity that varies as a function of shell height and the elevation angle of the LOS from receiver to satellite

$$\mathrm{Ob}(el, H) = \sec\left(\sin^{-1}\left(\frac{R_e}{R_e + H}\cos(\pi/2 - el)\right)\right) \tag{1}$$

where el is elevation angle, R_e is the radius of Earth, and H is the altitude of the thin shell (here taken to be 350km.) The obliquity factor ranges from a lower bound of one at zenith to a maximum around three for the chosen H. Using this approximation, GPS observations of ionospheric delay along any LOS can be converted to an equivalent vertical delay, $I_v = I_s/\mathrm{Ob}(el, H)$, where the so-called slant observation, I_s, is made directly by the receiver. The slant to vertical transformation is applied at the ionospheric pierce point (IPP) which is the intercept of the LOS ray and the thin shell at altitude H.

Figure 2 is a graphical depiction of the way this thin shell model is represented in the WAAS correction stream. As prescribed in the WAAS minimum operational performance standard (MOPS) [4] the thin shell model is sampled on a regularly spaced grid along latitude and longitude. These vertices are called ionospheric grid points (IGPs). The important features in Figure 2 are the triangles, crosses, and circles/diamonds. The triangles indicate reference stations where receivers gather observations of the ionosphere. The crosses are the IPPs where measurements of I_v are interpreted. The circles/diamonds are ionospheric grid points where the ionospheric model is estimated/not monitored.

Under the thin shell model the estimation problem is to take the measurements at IPPs (crosses) and form

vertical delay estimates at the IGPs (circles). For each grid point the WAAS system estimates a vertical ionospheric delay, I_v(IGP), and a confidence bound, GIVE(IGP), on the that delay estimate. The spatial correlation structure is critically important in generating both quantities, I_v and GIVE.

Conceptually one can think of the ionospheric correlation function as a cookie cutter. The estimators job is to apply it by first centering on an IGP and then including any IPPs that fall within the perimeter into the estimation. The profile of the cookie cutter is the correlation structure of the ionosphere and the radius (not necessarily uniform in all directions) serves as a monitor cut off.

The spatial correlation function is one of the two quantities the estimator can use to determine how much or little any given IPP measurement should contribute to an IGP. The other quantity being the confidence bound on the IPP measurement itself. An important point in our characterization will be the ability to keep these two quantities distinct and separable in the estimation problem. When the correlation structure is applied as a monitor the ionospheric correlation function is an indicator to the system when an IGP is not monitored (no IPPs included). In Figure 2 this information is captured by the distinction of an IGP as a circle (monitored) versus a diamond (not monitored).

As a starting point for identifying this spatial correlation function we turn to the reference station measurements themselves. As isolated observations the dual-frequency reference station measurements (code or carrier) are not suitable for our purpose. The noise and biases corrupting the ionospheric measurements will heavily distort the correlation structure of the ionosphere. We do not want to include these error sources within the correlation function and therefore require iron clad slant measurements. We do however want to include the deficiencies in the thin shell model as part of the correlation function. Thus we first eliminate the noise and biases to achieve truth, I_s, measurements and then transform those truth measurements into the vertical equivalents, I_v, of the thin shell model.

The process for obtaining truth I_s measurements relies on the complementary nature of the code and carrier GPS observations as well as geographical redundancy in the reference network. Three levels of pre-processing are applied to the raw GPS code and carrier observations in this process. First, the receiver and satellite hardware biases are calibrated in software [7, 1] using a multi-day collection of observations and removed from the raw code and carrier differences for every receiver satellite pair. Second, the code measurements for each continuous carrier phase track are matched to the carrier phase measurements.and averaged to resolve the carrier phase cycle ambiguity [10]. Finally, the resolved carrier phase tracks from the three receivers at any one location are compared to remove any faulty measurements [11]. The resulting truth vertical ionosphere at a given point in time is then average of fault-free measurements divided by the associated obliquity factor.

The truth process is summarized the following three steps:

1. Hardware bias removal (per code measurement)

$$I_\rho = \rho_{L2} - \rho_{L1} - \text{IFB} - \tau_{gd} + \xi_{L1L2} \qquad (2)$$

   where ρ is the raw code measurement on L1 and L2 respectively, IFB is the receiver hardware bias, τ_{gd} is the satellite hardware bias, and ξ_{L1L2} is the noise on the L1/L2 code difference.

2. Cycle ambiguity resolution (per phase track)

$$I_s = I_\phi - \frac{1}{M}\sum_{m=0}^{M}(I_\phi - I_\rho) \qquad (3)$$

   where M includes all observations in a continuous phase track.

3. Truth determination (per reference station)

$$I_v = \begin{cases} \frac{I_{s_1}+I_{s_2}+I_{s_3}}{3\text{Ob}(H,el)} & \text{if } |I_{s_i} - I_{s_j}| < T \ \forall i,j = 1..3 \\ \frac{I_{s_1}+I_{s_2}}{2\text{Ob}(H,el)} & \text{if } |I_{s_i} - I_{s_j}| < T \ \forall i,j = 1..2 \\ \text{NA} & \text{otherwise} \end{cases} \qquad (4)$$

   where T (nominally 30cm) is the detection threshold for rejecting faulty ionospheric measurements.

Figure 3 depicts 24 hours of real I_v measurements taken on 6 December 1999 and processed by Raytheon Systems Corporation and JPL. These measurements are the result of comparing three independent threads of geographically redundant post-processed GPS I_s measurements. The horizontal spread around 1500 UT is primarily due to the longitudinal distribution of the network which is

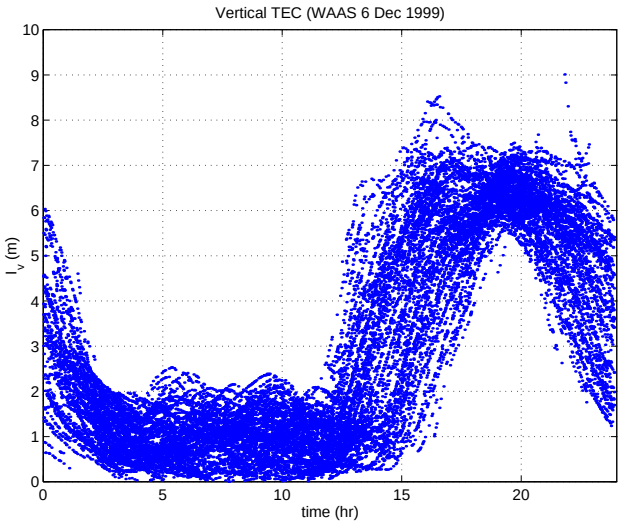

Figure 3: GPS measurements of the vertical equivalent ionospheric delay are made continuously by the WAAS reference network. The measurements above were taken on 6 December 1999 from the triply redundant reference network and post-processed to remove noise and bias errors. (Courtesy Raytheon Systems Corporation.)

rotating under the relatively stationary ionosphere in the solar-magnetic frame. The day-time peak here is around 7-8m which is indicative of the rising solar cycle, where only 12 to 18 months ago this peak was typically around 2-3m. Our correlation analysis will utilize these vertical ionospheric measurements as the raw resource for evaluating the correlation structure of.the vertical ionosphere.

CORRELATION MODEL

The main distinction in our construction of a spatial correlation function is that we analyze correlation of the thin shell ionosphere as an additive quantity rather than the more common treatment as a multiplicative quantity. There are three main reasons for this approach. The first is that we wish to characterize an absolute measure of the ionosphere instead of a relative scaling of its variation. The second is that the multiplicative approach incorrectly scales not only the ionospheric variation but the measurement noise as well. The third is that the additive correlation can be directly assessed on a point by point basis whereas the multiplicative correlation is based on a product over some finite interval of measurements which inherently smoothes the result.

As a practical matter the fundamental quantity in the additive approach is literally $|I_{v_i} - I_{v_j}|$ where i and j index IPPs (the crosses in Figure 2). In contrast, the fundamental quantity in the multiplicative approach is $\sum_{(i,j)} I_{v_i} I_{v_j}$ which is then normalized over the desired interval defined by the collection of pairs (i, j) to produce some function of distance between IPPs. The analogy in statistical analysis is that the additive approach samples the difference between realizations of a random variable and the multiplicative approach samples the convolution of their distributions. In theory these two approaches are equivalent but in practice, with real data, the former is much more definitive. Further, the latter is highly sensitive to the normalization step which is ad hoc at best.

Using this additive form for the ionospheric correlation structure yields a function of separation distance that can be directly applied to the determination of confidence bounds on the ionospheric corrections. Our approach relies on off-line post-processing of GPS measurements from the same sensors that are used to generate the ionospheric corrections in real-time. This is very beneficial because we do not need to make any assumptions about the sensors or models. The decorrelation function (reciprocal of the correlation function) can therefore be rigorously minimized to increase availability and yet still protect the user's navigation solution.

The identification process of the decorrelation function is relatively straightforward given a set of truth measurements, I_v, from the reference network described in the previous section. At each epoch, compute the difference between all I_v measurements and index them by the great circle distance between the IPPs where those measurements were made. Now form a two dimensional histogram as in the left graphic of Figure 4 where the horizontal axis is cut into bins of great circle distance (GCD) and the vertical axis, bins of $\Delta I_v = |I_{v_i} - I_{v_j}|$. It is clear from this difference calculation why the noise and bias errors would corrupt the correlation structure. Each entry in the histogram of Figure 4 then counts the number of times an ordered pair $(d, \Delta I_v)$ fell within that bin. Note that the color scale is logarithmic so that the largest bin counts are on the order of 100,0000 hits. For reference the bin sizes here are 25cm and 100km and the distance axis spans nearly two-thirds the width of CONUS.

The structure of the resulting histogram fits well with intuition. At shorter GCDs the difference between two I_v measurements is likely to be smaller than at

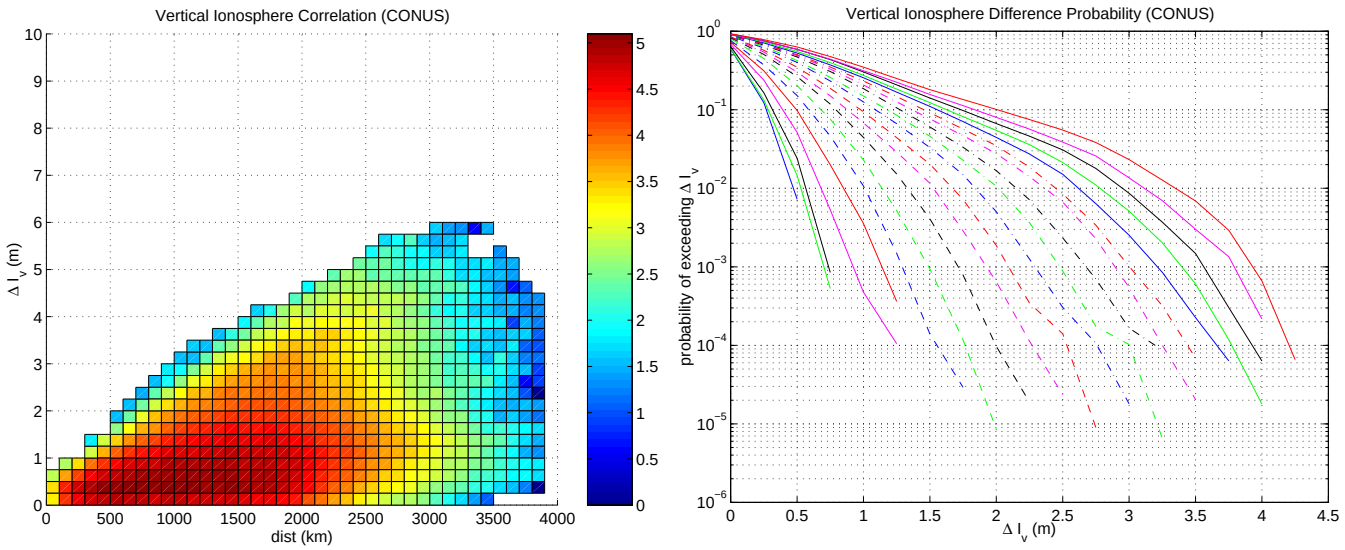

Figure 4: The two dimensional histogram (left graphic) of vertical ionospheric differences v. pierce point great circle separation shows the clean correlation structure of the ionosphere expected in CONUS. The family of cumulative likelihood curves (right graph) shows the occurrence rate of a given difference for each distance bin. Importantly, left-most line corresponds to 100km with curves increasing to the right-most at 2000km and so indicating monotonic growth.

longer GCDs. However there are some remarkable features, the most notable is the cleanliness of the distribution. There are no differences greater than 5m in the region where we have a statistically significant sampling and none greater than 6m over the entire region of interest. Also it appears that the intercept is non-zero which is reasonable when considering the imperfections of the thin shell model. We believe that the non-zero offset is indeed due to the thin shell model and not to residual noise in the measurements, I_s. In a cursory confirmation of the truth measurements at five reference stations, the residual differences between fault-free I_s measurements along any given LOS were on the order of 5cm. Although additional examination may be warranted for completeness, the obliquity error in (1) will definitely be present and in our opinion dominate any residual measurement error.

The right graphic in Figure 4 interprets the two dimensional histogram by plotting the cumulative likelihood of ΔI_v occurrence for each distance bin, one curve per bin. The family of curves can be used manually to look up the likelihood that at two points separated by some GCD on the thin-shell ionospheric the difference between two I_v measurements will be below some value. For example, 99% of the time under nominal two IPPs separated by 2000km on the great circle at 350km altitude will have I_v measurements that differ by 3.5m or less.

The regularity in the two degrees of freedom (distance and difference) in the graphs of Figure 4 provides a convenient way to collapse the decorrelation function into a one dimensional function. While the two dimensional histogram is instructive, it can be condensed further into a functional form that is much more useful.

The curves in Figure 5 demonstrate the regularity of the ionosphere captured in the two dimensional histogram. Here we have picked off the ΔI_v corresponding to various percentile levels, 68%, 95%, 99%, and 99.9%, and translating it to an equivalent standard deviation (divide by 1, 2, 2.57, and 3.29 respectively) The dramatic result of this operation is that all four of these fall on the same track. This means that the distribution of I_v differences in any distance bin is well modeled by a gaussian. Further, the decorrelation function is affine with distance having an intercept around 0.5m and a slope of 0.5m/Mm. Thus we have a very usable form for the additive decorrelation function, which we call, $r(\mathrm{GCD})$

$$r = b + m\mathrm{GCD}) \tag{5}$$

where b is the intercept at 0.5m, m is the slope of 0.5m/Mm and GCD is again great circle distance.

Given this functional form for the decorrelation of the thin-shell ionosphere we can implemented the two part cookie cutter weighting function mentioned in

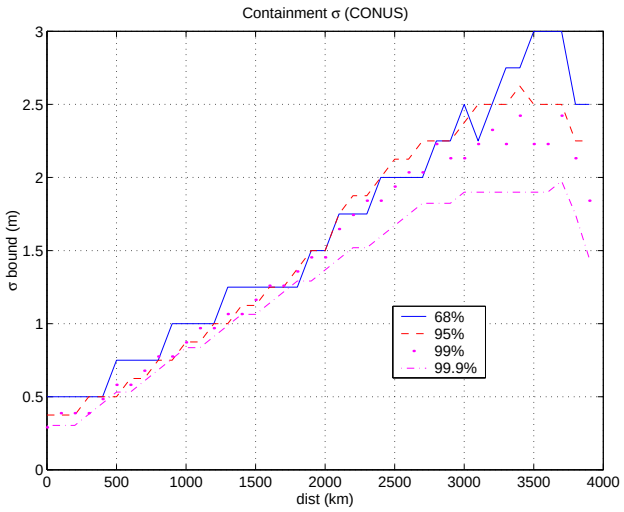

Figure 5: The standard deviation indicated by each of the given percentile counts are plotted as a function of GCD. The dramatic result is that the 68%, 95%, 99%, and 99.9% intervals all map back to the same standard deviation. This indicates that the occurrence of I_v differences in any distance bin is well modeled by normal distribution.

the modeling section

$$w_{ij} = \begin{cases} \frac{1}{\sigma_I + r} & \text{if } GCD <= D \\ 0 & \text{if } GCD > D \end{cases} \qquad (6)$$

where σ_I is the confidence bound on the real-time I_v measurement (not post-processed truth) and D is the radius up to which statistical significance holds in the sampling of the histogram of Figure 4. Here D was taken to be 1700km. In the next section we conduct a preliminary evaluation of the system performance when using this additive decorrelation function in estimation and monitoring process of generating the corrections, I_v(IGP), and confidence bounds, GIVE(IGP).

We close this section by qualifying the result to this point. The correlation structure was analyzed on a relatively quiet, geomagnetically speaking, day over CONUS. We are in the process of evaluating the same correlation analysis on measurements taken during ionospheric storm conditions and with wider geographic distribution. The obvious steps to be explored once that data is processed are to parameterize the additive correlation function over geomagnetic latitude, solar conditions, and geomagnetic activity.

PERFORMANCE

Given a model for the nominal correlation structure of the ionosphere as represented by the thin-shell approximation we would like to test the ionospheric correction process against real data. Expecting to achieve very good performance under nominal conditions, performance in the presence of threat conditions, those which violate the decorrelation function, is critical from the perspective of safety. Toward this end we have realized a threat scenario based upon an extreme disturbance observed by the incoherent scatter radar at Millstone Hill in Westford, MA [12, 13]. This disturbance was added onto real data collected by the National Satellite Test Bed (NSTB) in June of 1998 which was in turn injected to the estimation process outlined above.

This disturbance, depicted in the two pictures of Figure 6, propagated southward across the Northeast United States over a period of 6-7hrs. The manifestation of this storm enhanced plasma density (SED) is shown in the I_s time history of Figure 7. There the time history of the range delay (top trace) seen by the reference receiver at Ottawa, Ontario viewing PRN 18 has a dramatic increase around an hour into the track as the LOS passed through the SED. As expected the WAAS correction (second trace from top) cannot reproduce this disturbance because the SED is too geographically localized for the WAAS grid to capture it. However we see that the σ confidence bound (bottom) trace is sensitive to the disturbance through a χ^2 feedback test and adequately covers the residual error (second trace from bottom). We say that the residual error is covered when it is contained by the 5.33σ trace.

While it is instructive to examine the performance in the pseudorange domain as above, the real evaluation occurs in the position domain where all three of the WAAS corrections (clock, ephemeris, ionosphere) are applied to form a differentially corrected navigation fix. The critical. The three primary performance metrics for the WAAS navigation solution are accuracy, integrity, and availability all of which are quantified in the triangle charts of Figure 8. These charts are two dimensional histograms reporting the occurrence of the ordered pair (vertical protection limit,vertical error). Accuracy is quantified on the horizontal axis, availability is quantified on the vertical axis, and lack of integrity is indicated by points falling below the diagonal. For a full interpretation of the triangle chart the interested reader is directed to Walter [14]. Succinctly put, the desired outcome is for all points to fall in the white

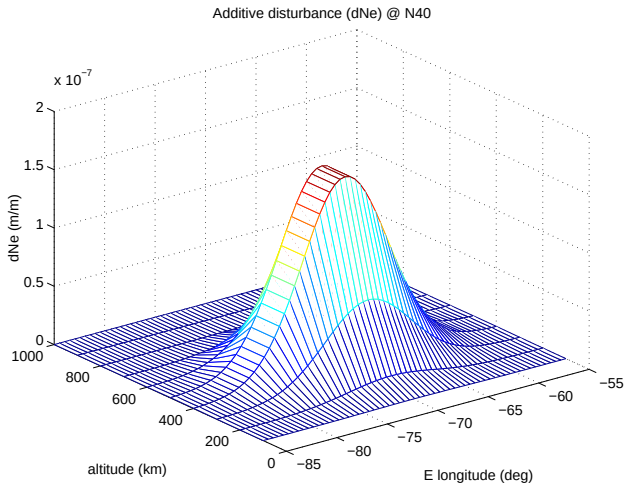

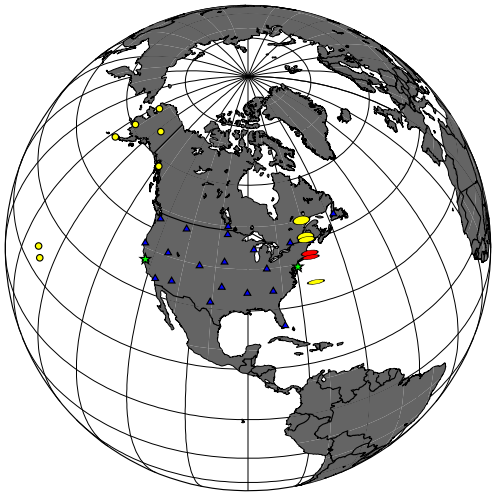

Figure 6: An electron density disturbance was synthesized from observations made by the Millstone Hill incoherent scatter radar in Westford, MA on 8 February 1986. The disturbance was a storm enhanced plasma density (SED) that propagated southward along the West 70° meridian. This intense disturbance has equates to maximum TEC variations on GPS observations of up to 6m over distances of a few hundred kilometers.

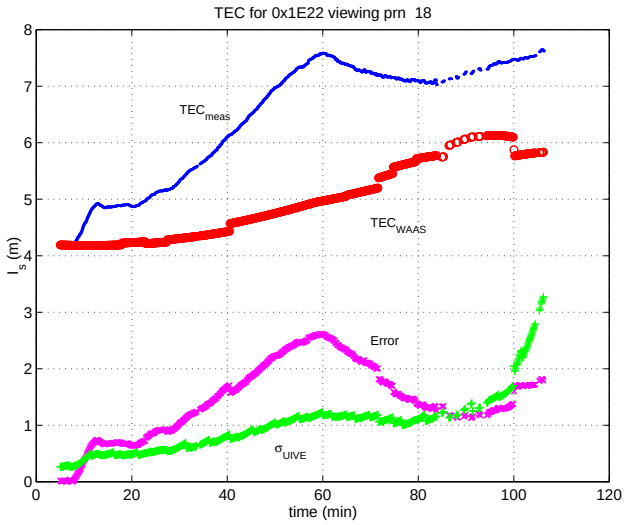

Figure 7: The response to the ionospheric SED disturbance is a rapid increase in delay on the time history of the I_s observations. Here the static user located at Ottawa, Ontario was viewing PRN 18 through the disturbance.

triangle bounded below by the 45 and above by the vertical alert limit (VAL) which is here taken to be 12m for CAT1 operations.

For comparison, the two charts on the left of Figure 8 report the performance of the system under nominal conditions at Ottawa, Ontario and Atlantic City, New Jersey. On the right are the same two user's but now experiencing the disturbance condition. These two users were the most effected by the disturbance. While the disturbance clearly had an effect.on the positioning results the ability of the system to isolate and protect against this disturbance is borne out in the triangle charts. Widely regarded as the most severe ionospheric disturbance recorded in CONUS, the system performance using this correlation structure in the face of the 8 February 1986 storm is compelling. The basic result here is that localized disturbances are neither a safety threat because the reference network is capable of catching the disturbance and increasing the error bounds where it cannot correct the delay. Further, if the satellite constellation geometry is strong then these types of localized disturbances are not disruptive to service. The disturbed LOSs are effectively removed by deweighting their contribution to the navigation solution via an increased GIVE.

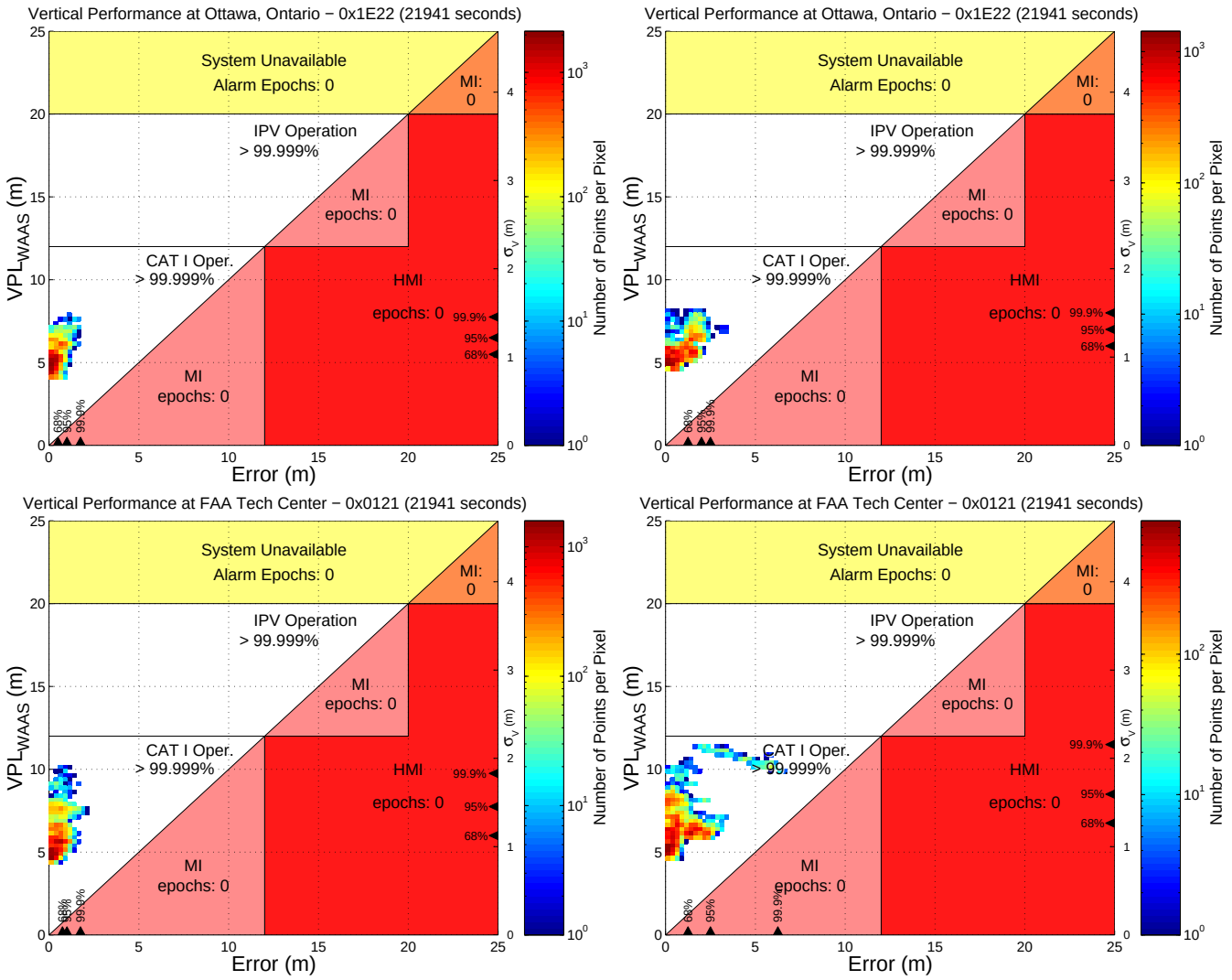

Figure 8: WAAS user positioning performance in the form of accuracy, integrity, and availability is measured every epoch. In the left column are the triangle charts for the nominal 12 hour period. In the right column are the triangle charts for that include the disturbance model that was based on the 8 February 1986 ionospheric phenomenon observed by the incoherent scatter radar located at Millstone Hill in Westford, MA.

CONCLUSIONS

The WAAS grid, when coupled with an accurate decorrelation model, provides a viable covariance based error bounding mechanism for generating GIVE protections bounds. Likewise, the decorrelation function also provides a physically based thresholding scheme for integrity monitoring of IGPs. The additive correlation model presented here was determined from real WAAS reference station measurements demonstrating that all the necessary resources are available to the WAAS system for implementing such an identification process on a continuous basis.

The basic requirement for carrying out a reliable characterization is the collection of redundant GPS observables needed to remove measurement noise, biases, and faulty measurements. The resulting decorrelation function serves a dual role as both a contributor to the weighting function and indicator for the monitoring function.

Synthetic disturbances and real data were used here for verification of the integrity processing under stressful ionospheric conditions. Eventually real storm and geographically diverse measurements will be needed to fully validate the model. Likewise a better understanding of the spatial and temporal correlation structure of the residual correction error will aid in improving the availability of the system.

ACKNOWLEDGMENTS

The authors wish to thank Jack Klobuchar for his helpful discussions and insight during the research process leading to this paper. We also thank the FAA Technical Center, Francois Choquette of Raytheon Systems Corporation and Dr. Byron Iijima of the Jet Propulsion Laboratory for supplying raw data and the post-processed measurement data from the WAAS reference network. We gratefully acknowledge the FAA Satellite Navigation Program Office for sponsoring the WAAS/GPS research at Stanford.

REFERENCES

[1] A. J. Hansen, "Real-time ionospheric tomography using terrestrial GPS sensors," *Proceedings of the Institute of Navigation GPS-98*, September 1998. student competition winner.

[2] P. Enge, "WAAS messaging system: Data rate, capacity, and forward error correction," *Navigation*, vol. 44, pp. 63–76, Spring 1997.

[3] A. J. Hansen, Y.-C. Chao, T. Walter, and P. Enge, "Ionospheric estimation and integrity threat detection," *Proceedings of the Institute of Navigation National Technical Meeting*, pp. 883–9, January 1997.

[4] RTCA Special Committee 159, *Minimum Operational Performance Standards for Airborne Equipment Using Global Positioning System/Wide Area Augmentation System*, RTCA/DO-229 Change 3, November 1997.

[5] B. W. Parkinson and J. J. Spilker, eds., *Global Positioning System: Theory and Application.* Washington, D.C.: AIAA, 1996.

[6] R. S. Conker, M. B. El-Arini, T. W. Albertson, J. A. Klobuchar, and P. Doherty, "Development of real-time algorithms to estimate the ionopsheric error bounds for WAAS," *Proceedings of the Institute of Navigation GPS-95*, pp. 1247–58, September 1995.

[7] B. D. Wilson and A. J. Mannucci, "Instrumental biases in ionospheric measurements derived from GPS data," *Proceedings of the Institute of Navigation GPS-93*, pp. 1343–51, September 1993.

[8] D. Bilitza, K. Rawer, L. Bossy, and T. Gulyaeva, "International reference ionosphere–past, present, future," *Advances in Space Research*, vol. 13, no. 3, pp. 3–23, 1993.

[9] R. E. Daniell and et. al., "A global ionospheric parameterization based on first priciples models," *Radio Science*, vol. 30, no. 3, pp. 1499–1510, 1995.

[10] "Private conversation with dr. byron iijima," January 2000. JPL.

[11] "Private conversation with fracois choquette," January 2000. Raytheon Systems Corporation.

[12] J. C. Foster, "Storm time plasma transport at middle and high latitudes," *Journal of Geophysical Research*, vol. 98, pp. 1675–89, February 1993.

[13] J. C. Foster, "A quantitative investigation of ionospheric density gradients at mid latitudes," *Proceedings of the Institute of Navigation NTM-00*, January 2000.

[14] T. Walter, P. Enge, and A. J. Hansen, "An integrity equation for use in space based augmentation systems," *Proceedings of the DSNS*, March 1997.